Agricultural and Forest Meteorology 292–293 (2020) 108107

Contents lists available at ScienceDirect

Agricultural and Forest Meteorology

journal homepage: www.elsevier.com/locate/agrformet

Hydraulic safety margins of co-occurring woody plants in a tropical karst forest experiencing frequent extreme droughts

Feng-Sen Tan[a,1], Hui-Qing Song[a,1], Pei-Li Fu[b], Ya-Jun Chen[b], Zafar Siddiq[c], Kun-Fang Cao[a], Shi-Dan Zhu[a,*]

[a] State Key Laboratory for Conservation and Utilization of Subtropical Agro-bioresources, Guangxi Key Laboratory of Forest Ecology and Conservation, Guangxi University, Daxuedong Road 100, Xixiangtang District, Nanning, Guangxi 530004, China

[b] Key Laboratory of Tropical Forest Ecology, Xishuangbanna Tropical Botanical Garden, Chinese Academy of Sciences, Menglun Town, Mengla Country, Yunnan 666303, China

[c] Department of Botany, Government College University, Katchery Road, Lahore 54000, Pakistan

ARTICLE INFO

Keywords:
Cavitation
Extreme drought
Functional group
Liana
Minimum water potential
Vulnerability segmentation

ABSTRACT

Hydraulic safety margins (*HSM*) have been widely studied to assess the hydraulic risks and/or strategies of plant species under drought. However, calculations of *HSM* tend to vary between studies, leading to conflicting conclusions. In this study, *HSM* of 16 co-occurring woody species (including evergreen trees, brevi-deciduous trees, and lianas) in a tropical karst forest was investigated. They were expressed as: (1) the difference between minimum leaf water potential and water potential causing 50% loss of leaf hydraulic conductance (HSM_{leaf}), (2) the difference between water potential at stomatal closure and that at 50% loss of branch hydraulic conductivity (HSM_{stomatal}), and (3) the difference between water potential at 50% loss of leaf hydraulic conductance and that at 50% loss of branch hydraulic conductivity ($HSM_{\mathrm{segmentation}}$). We asked the following questions: were HSM_{leaf} in the normal and extreme dry seasons across plant groups different? Were there correlations between different *HSM*-calculations? Results showed that, on average, the three plant groups showed similar and positive HSM_{leaf} in the normal dry season, but evergreen trees declined to a more negative value in the extreme dry season while the other two groups remained positive. The massive loss of leaf hydraulic conductance in several evergreen tree species was consistent with their extensive shoot dieback under extreme droughts. Across species, there were no significant relationships between HSM_{stomatal} and HSM_{leaf}. Most species (mainly lianas and brevi-deciduous trees) showed negative $HSM_{\mathrm{segmentation}}$, which did not support the vulnerability segmentation hypothesis that branches are more resistant to cavitation than leaves. Moreover, more negative $HSM_{\mathrm{segmentation}}$ tended to have lower HSM_{stomatal} and larger HSM_{leaf} in the extreme dry season. This study indicates that karst evergreen trees are more likely to experience leaf hydraulic failure under extreme droughts, and reveals potential correlations between branch and leaf hydraulic safety strategies. Further studies on HSM-demographic rate relationship in the tropical karst forests are recommended.

1. Introduction

Droughts are one of the most significant environmental limitations for plant growth and survival (Lambers et al., 2008). Due to global climate change, shifts in rainfall patterns and increasing temperatures have increased the frequency and severity of droughts in many regions, particularly in tropical regions (Zhang et al., 2007; Feng et al., 2013). Furthermore, widespread forest decline caused by extreme drought stress around the world has been observed over the past decades, which exerts a profound effect on the structure and function of forest ecosystems (Allen et al., 2010; Booth et al., 2012; Anderegg et al., 2013). An important eco-physiological mechanism underlying tree dieback or mortality is the failure of the hydraulic transport systems due to severe cavitation (McDowell et al., 2008; Nardini et al., 2013; Rowland et al., 2015; Choat et al., 2018; Liu et al., 2018).

Hydraulic safety margin (*HSM*) can assess the degree of plant's hydraulic risks and/or qualify hydraulic strategies during drought periods, which have been widely studied in the field of plant physiological ecology (Klein et al., 2014; McCulloh et al., 2015; Anderegg et al., 2016; Johnson et al., 2018). There are several ways to determine *HSM*:

---

[*] Corresponding author.
E-mail address: zhushidan@gxu.edu.cn (S.-D. Zhu).
[1] These two authors contributed equally to this work.

https://doi.org/10.1016/j.agrformet.2020.108107
Received 9 February 2020; Received in revised form 9 June 2020; Accepted 12 July 2020

(1) the difference between minimum leaf water potential and water potential at 50% loss of leaf hydraulic conductance (*HSM_{leaf}*), or between the minimum xylem water potential and the water potential at 50% loss of branch hydraulic conductivity (*HSM_{branch}*). A narrower value indicates that the plant organs operate at a water potential closer to the threshold of hydraulic dysfunction (Meinzer et al., 2009; Delzon and Cochard, 2014). Previous studies have shown that *HSM_{leaf}* could be an index of drought-induced damage under natural droughts for co-occurring tree species (Skelton et al., 2017a; Zhang et al., 2017; Powers et al., 2020). (2) *HSM* can be calculated as the difference between the water potentials at stomatal closure during seasonal drought and that at 50% loss of branch hydraulic conductivity (stomatal safety margin; *HSM_{stomatal}*). Timely stomatal closure avoids the excessive decline of water potential and thus contributes to a larger safety margin in branches (Brodribb and Holbrook, 2004; Skelton et al., 2015; Martin-StPaul et al., 2017; Blackman et al., 2019). Previous studies have found that the slope of the linear relationship between leaf water potential at turgor loss point (Ψ_{tlp}) and that at stomatal closure is close to one (Bartlett et al., 2016; Martin-StPaul et al., 2017). Using Ψ_{tlp} as a proxy for leaf water potential at stomatal closure can provide a rapid way to quantify stomatal regulation strategy (Martin-StPaul et al., 2017; Ziegler et al., 2019). (3) *HSM* can be calculated as the difference between water potentials at 50% loss of leaf hydraulic conductance and that at 50% loss of branch hydraulic conductivity, which is also termed as vulnerability segmentation (*$HSM_{\mathrm{segmentation}}$*; Tyree et al., 1993; Bucci et al., 2013; Nolf et al., 2015). Unlike *HSM_{leaf}* that is strongly influenced by environmental water conditions (water potential), *$HSM_{\mathrm{segmentation}}$* seems to be more inherent and static for a plant species. A classic vulnerability segmentation hypothesis proposes that leaves are more vulnerable to cavitation than branches, and a strong leaf to branch vulnerability segmentation (large *$HSM_{\mathrm{segmentation}}$*) enables leaves to act as safety valves to protect the main hydraulic pathway from dysfunction (Choat et al., 2005; Johnson et al., 2011; Pivovaroff et al., 2014).

Several studies using different definitions of *HSM* have reported conflicting results. For example, based on the global meta-analysis, Choat et al. (2012) found that most of the angiosperm species operated at a narrow *HSM_{branch}* (< 1 MPa), but Martin-StPaul et al. (2017) reported a large *HSM_{stomatal}* for most woody plants with high interspecific variation. However, other studies have revealed significant correlation between different definitions of *HSM*; for example, between *$HSM_{\mathrm{segmentation}}$* and *$HSM_{\mathrm{leaf}}$* (Johnson et al., 2016; Zhu et al., 2016), or between *HSM_{stomatal}* and *HSM_{branch}* (Skelton et al., 2015). Hence, characterizing *HSM* based on multiple plant organs and mechanisms and exploring their correlations may give us a full understanding of a plant's resistance and overall hydraulic response to drought stress (Johnson et al., 2016; Fontes et al., 2018; Wason et al., 2018). This is particularly imperative in high biodiverse ecosystem regions experiencing frequently extreme droughts, where plant species exhibit a broad range of drought survival strategies (Pivovaroff et al., 2018).

Karst forest ecosystems are extensively distributed in tropical regions in southwestern China, where are biodiversity hotspot and conservation priority because of the presence of many endemic plant species (Yuan, 1991; Zhu et al., 2003). The karst habitats are characterized by many rock outcrops, shallow and patchy soils, and fast subterranean drainage and overland flow (Zhu et al., 2003; D.Y. Fan et al., 2011). Therefore, tropical karst species frequently suffer from drought due to limited water availability, especially during the hot-dry season (Fu, 2011; Zhu et al., 2017). Several previous studies have reported that co-occurring tropical karst species or functional groups present different hydraulic strategies to cope with seasonal drought. For example, Fu et al. (2012) found that evergreen trees were more drought-tolerant than brevi-deciduous trees in a tropical karst forest, with higher wood density, lower turgor loss point and greater resistant to cavitation. In another study at the same site, Chen et al. (2015) found that despite being more vulnerable to cavitation, lianas can access deeper soil water sources and exhibit stronger physiological adjustments compared to co-occurring trees. From 2008 to 2012, the seasonal drought became more severe in this region of China because of the influence of El Niño events (Qiu, 2010). Such extreme droughts provide unique natural conditions to assess inter-specific hydraulic responses to future climatic change (Nardini et al., 2013; Johnson et al., 2018).

In the present study, we measured pressure-volume relations, vulnerability curves of branches and leaves, wood density (ρ_{sapwood}) and saturated water content (SWC) in a normal dry season for 16 co-occurring woody species in a tropical karst forest, and monitored their minimum leaf water potential through the normal and extreme dry seasons. These species belong to three plant groups, i.e., brevi-deciduous trees (a short leaf-shedding period in the dry season), evergreen trees, and lianas. We calculated their *HSM_{leaf}* under normal and extreme droughts, respectively, as well as *HSM_{stomatal}* and *$HSM_{\mathrm{segmentation}}$*. Our objectives were to: (1) investigate the differences in *HSM_{leaf}* between the normal and extreme dry seasons across species and plant functional groups, (2) identify which hydraulic traits (i.e., Ψ_{tlp}, ρ_{sapwood}, and SWC) were associated with *HSM_{leaf}* under extreme droughts, and (3) explore the correlations between different *HSM*-calculations.

2. Materials and methods

2.1. Study site and plant materials

This study was carried out in a tropical karst forest in Xishuangbanna Tropical Botanical Garden, southwestern China (21°54′ N, 101°46′ E; 600–650 m a.s.l.). This area is strongly influenced by a monsoon climate and thus has a distinct dry season from October to April. According to long-term meteorological data (more than 50 years) as recorded at a nearby weather station 3 km northwest from the study site, the mean annual precipitation is about 1550 mm, 80% of which occurs during the wet season (May to September). The mean annual temperature is 21.4 °C, with monthly temperatures ranging from 14.8 °C (January) to 25.5 °C (July). From 2008 to 2012, several extreme drought episodes during the dry season occurred at this site, for example, the total precipitation from Dec. 2011 to Mar. 2012 was 22 mm, which was approximately a fifth of the precipitation during that period in a normal dry season (Fig. 1).

The karst forest at this site is dominated by evergreen tree species such as *Cleistanthus sumatranus* (Miq.) Muell. Arg., *Celtis philippensis* Blanco, and *Lasiococca comberi* Haines, mixed with brevi-deciduous tree species (e.g., *Lagerstroemia tomentosa* Presl, *Croton crassifolius* Geisel., and *Ficus pisocarpa* Bl.) because of the dry habitat (Zhu et al., 2003). The brevi-deciduous tree species have a short leaf-shedding period (two to three months) in the mid-dry season, followed by a flush of new leaves at the end of the dry season. During extreme drought events, leaf desiccation and/or shoot dieback of several canopy dominant evergreen tree species were recorded (Fig. S1; Fu, 2011). Sixteen common tree and liana species from the karst forest were investigated in the present study (Table 1). They are angiosperms, except for *Gnetum montanum* Markgr. that is a gymnosperm liana species with angiosperm-like traits such as broad leaves and vessels. For each species, four to five healthy adult individuals were selected for the measurements (Table 1). No lianas were attached to the trees that were selected. All the branch and leaf hydraulic traits were measured in a normal dry season after the 2008–2012 extreme droughts, except for leaf water potential that was monitored over a long-term.

2.2. Midday leaf water potential in the dry season

We have been monitoring midday leaf water potential (Ψ_{min}) in the late-dry season (March to April) from 2008 to the present, through both normal and extreme dry seasons ($\Psi_{\mathrm{min\_normal}}$ and $\Psi_{\mathrm{min\_extreme}}$). Between 12:00 and 14:00 on continuously sunny days, 10 sun-exposed branches bearing fully expanded and healthy leaves from four to five mature

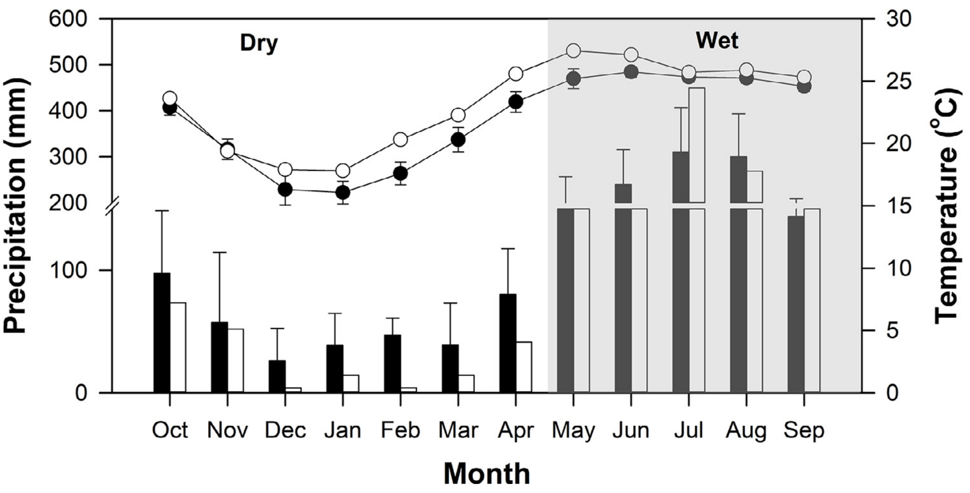

Fig. 1. Monthly precipitation (*bars*) and average atmospheric temperature (*circles*) of long-term data (1959–2015; *black*) and during Oct. 2011–Sep. 2012 (*white*). Precipitation shows average monthly values for long-term data and total values for Oct. 2011–Sep. 2012. The wet season (*gray*) lasts from May to September.

individuals per species were collected. After excision, leaf water potential was immediately determined using a pressure chamber (PMS, Corvallis, OR, USA).

2.3. Pressure-volume relation

To avoid the effect of oversaturation due to overnight rehydration on pressure-volume curves, leaf-bearing branches were sampled early in the morning (on rainy days) in a normal dry season, placed in a plastic black bag with moist towels, and immediately transferred to the laboratory within half an hour for further measurements. For each leaf sample, leaf mass and water potential were measured periodically during desiccation under laboratory conditions. Finally, leaf dry mass after oven-drying at 70 °C for at least 48 h was measured by an analytical balance (ML204T, Mettler Toledo, Zurich, Switzerland) with the precision at 0.0001 g. Leaf turgor loss point (Ψ_{tlp}) and slopes of pressure-volume relationship were calculated from a P-V curve fitting program (Schulte and Hinckley, 1985). Given that there is a close relationship between Ψ_{tlp} and leaf water potential at stomatal closure (Brodribb et al., 2003; Bartlett et al., 2016; Martin-StPaul et al., 2017; Tureba et al., 2019), we used Ψ_{tlp} as a surrogate for leaf water potential at stomatal closure in this study.

2.4. Leaf hydraulic vulnerability curve

The rehydration kinetics method was used to establish leaf hydraulic vulnerability curves, which described the response of leaf hydraulic conductance (K_{leaf}) to declining leaf water potential (Brodribb and Holbrook, 2003). For all the species, the collection of leaf-bearing branches and transfer to a close-by laboratory was similar to that for P-V measurements in an early dry season. To obtain a range of water potentials, these leaf-bearing branches were allowed to dry out slowly on the bench in the laboratory. Before determination of K_{leaf}, leaf-bearing branches were equilibrated by sealing in a black bag for about 1 h to ensure all the attached leaves had similar water potential, i.e., the difference between two leaves from apical and basal of each branch was less than 0.1 MPa. After the measurement of initial water potential of equilibrated leaves (Ψ_0), neighboring leaves were cut under-water and allowed to rehydrate for 10–200 s (t). The rehydration time was chosen by allowing the water potential of the rehydrated leaves (Ψ_f) to be about half of the Ψ_0. Leaf hydraulic conductance was calculated using the following equation (Brodribb and Holbrook, 2003): $K_{leaf} = C \times \ln(\Psi_0/\Psi_f)/t$, where C is leaf capacitance and was calculated as follows: $C = \Delta RWC/\Delta\Psi_L \times (DM/LA) \times (WM/DM)/M$, where $\Delta RWC/\Delta\Psi_L$ before or after turgor loss point was calculated from the slopes of leaf pressure-volume relationships, DM (g) is leaf dry mass, LA (cm^2) is leaf area, WM (g) is mass of leaf water at 100% relative leaf

Table 1

The 16 tree and liana species sampled in this study. Four to five individuals for each species were selected, and the ranges (mean values) of height and diameter at breast height (DBH) were measured. The liana species were mature individuals that reached the canopy. * indicates extensive leaf desiccation and/or shoot dieback occur under extreme drought (Fu, 2011).

Species	Family	Growth	Leaf habit	Leaf texture	Height (m)	DBH (cm)
Alphonsea monogyna Merr. et Chun	Annonaceae	Tree	Evergreen	Leathery	9–12 (11.8)	13–33 (22.3)
Celtis philippensis Blanco*	Ulmaceae	Tree	Evergreen	Leathery	13–22 (14.5)	20–51 (37.5)
Cleidion bracteosum Gagnep.	Euphorbiaceae	Tree	Evergreen	Leathery	5–7 (5.7)	9–15 (12.2)
Cleistanthus sumatranus (Miq.) Muell. Arg.*	Euphorbiaceae	Tree	Evergreen	Leathery	6–7 (6.5)	16–27 (20)
Pistacia weinmannifolia J. Poisson ex Franch.	Anacardiaceae	Tree	Evergreen	Leathery	5–8 (6.3)	21–36 (28.3)
Lasiococca comberi Haines*	Euphorbiaceae	Tree	Evergreen	Leathery	6–12 (8.5)	14–18 (16.3)
Turpinia pomifera (Roxb.) DC.	Staphyleaceae	Tree	Evergreen	Leathery	5–11 (8.0)	10–27 (16.9)
Cipadessa baccifera (Roth.) Miq.	Meliaceae	Tree	Brevi-deciduous	Papery	4–8 (5.5)	12–31 (19.7)
Croton crassifolius Geisel.	Euphorbiaceae	Tree	Brevi-deciduous	Papery	7–10 (8.4)	13–24 (17.9)
Ficus pisocarpa Bl.	Moraceae	Tree	Brevi-deciduous	Papery	4–6 (5.0)	12–22 (15.5)
Lagerstroemia tomentosa Presl	Lythraceae	Tree	Brevi-deciduous	Leathery	9–13 (11.6)	15–25 (22.3)
Mayodendron igneum (Kurz) Kurz	Bignoniaceae	Tree	Brevi-deciduous	Leathery	8–10 (9.0)	16–21 (19.4)
Bauhinia touranensis Gagnep.	Fabaceae	Liana	Evergreen	Leathery		6–7 (6.4)
Combretum latifolium Bl.	Combretaceae	Liana	Brevi-deciduous	Leathery		8–20 (12.9)
Gnetum montanum Markgr.	Gnetaceae	Liana	Evergreen	Leathery		4–7 (4.7)
Ventilago calyculata Tulasne	Rhamnaceae	Liana	Evergreen	Leathery		7–19 (9.8)

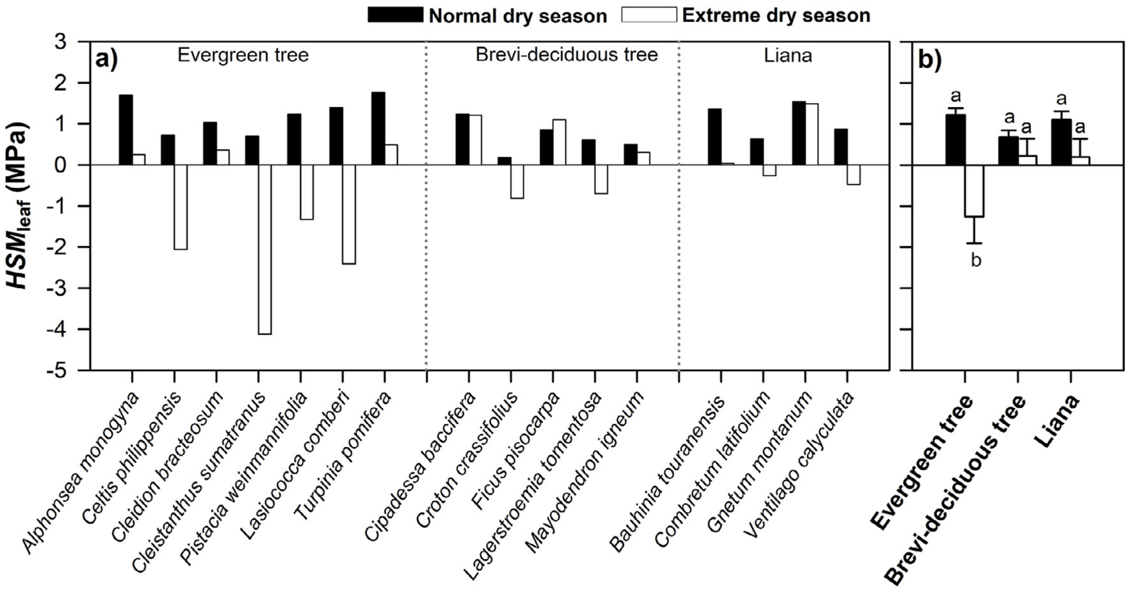

Fig. 2. Mean leaf hydraulic safety margins (*HSM_{leaf}*) of the 16 woody species during the normal (*black*) and the extreme dry seasons (*white*). *HSM_{leaf}* is calculated as the difference between minimum leaf water potential in the dry season and that at 50% loss of leaf hydraulic conductance. Data are means ± SE for each plant group. Different letters denote significant differences ($P < 0.05$).

water content (fresh mass–dry mass), and M is the molar mass of water (g mol^{-1}). Leaf hydraulic conductance was subsequently determined at different water potentials as described earlier. Leaf vulnerability curves were constructed by plotting K_{leaf} against Ψ_0, using a three-parameter sigmoid model in SigmaPlot 12.5 (Systat Software Inc., San Jose, CA, USA). Leaf water potential at 50% of maximum K_{leaf} ($P50_{leaf}$) was used to estimate the vulnerability of leaves to hydraulic dysfunction.

2.5. *Branch vulnerability curve*

Branch xylem vulnerability curves were determined using the bench-drying method (Sperry et al., 1988) in the normal dry season. The maximum vessel length (MVL) of these species has been reported by Zhu et al. (2017), ranging from 28 cm (*Pistacia weinmannifolia*) to 308 cm (*Bauhinia touranensis*). To avoid the artifact of cutting-induced cavitation (Wheeler et al., 2013), between 20 and 30 leaf-bearing branches longer than at least 2-times MVL (except for the liana species with long MVL) were collected from different individuals per species at predawn, stored in a big plastic black bag with moist towels and transported to the laboratory. These branch samples were allowed to dehydrate for different time periods (two days to a week). During the dehydration process, leaf water potential was periodically measured. Once the desired water potentials were approximately reached, whole branches were wrapped with plastic bags for 1–2 h to equilibrate. Water potentials of three leaves from the branch were then measured, the average value of which was equal to branch water potential (Ψ_{xylem}). Subsequently, one branch segment was cut underwater, removing about one MVL length (for tree species) or one fork (for liana species) from the base of the branch, and trimmed with a razor blade. Initial hydraulic conductivity (k_i) of the segment was measured using the steady-state flow-meter method (Sperry et al., 1988). After flushing with 20 mM KCl solution at a pressure of 0.1 MPa for 20–30 min, maximum hydraulic conductivity (k_{max}) of the branch segment was re-measured. Percentage loss of hydraulic conductivity (*PLC*,%) was calculated as: $PLC = 100 \times (k_{max} - k_i)/k_{max}$. The branch vulnerability curves were plotted using *PLC* as a function of Ψ_{xylem}. Xylem water potential at 50% loss of hydraulic conductivity ($P50_{stem}$) was calculated to describe vulnerability to cavitation.

2.6. *Sapwood density and saturated water content*

Wood samples were taken from the branch segments that were used for hydraulic measurements. After removing the bark and pith, the mass of fresh sapwood was measured, and the volume of the sample was determined by using the water displacement method. Then, the sample was oven-dried at 70 °C for 48 h and weighed again to obtain the dry mass. Sapwood density ($\rho_{sapwood}$, g cm^{-3}) was determined by dividing the dry mass by the volume of the sample. The sapwood saturated water content (SWC,%) was calculated as the ratio of saturated water mass to dry mass (Bucci et al., 2004).

2.7. *Calculations of hydraulic safety margins*

Leaf hydraulic safety margin in the normal dry season (HSM_{leaf_normal}) was calculated as the difference between Ψ_{min_normal} and $P50_{leaf}$, and in the extreme dry season ($HSM_{leaf\_extreme}$) was calculated as the difference between $\Psi_{min\_extreme}$ and $P50_{leaf}$ (McCulloh et al., 2015; Bucci et al., 2019). The stomatal safety margin ($HSM_{stomatal}$) was calculated as follows: $HSM_{stomatal} = \Psi_{tlp} - P50_{branch}$. The difference between water potential causing 50% loss of hydraulic conductance in leaves and branches was also a way to define hydraulic safety margin and calculated as $HSM_{segmentation} = P50_{leaf} - P50_{branch}$ (Bucci et al., 2013; Nolf et al., 2015).

2.8. *Statistical analysis*

We conducted a one-way analysis of variance (ANOVA) to compare the difference in leaf hydraulic safety margins in the normal and extreme dry seasons (Dependent variable) among the three plant groups (Factor), followed by post hoc pairwise comparisons based on the least significant difference (LSD) test. All the data were normalized prior to analysis to achieve normality, and statistical significance was recognized at $P < 0.05$. Correlations between each pair of traits were examined using the linear regression analyses (Pearson). All statistical analyses were performed using SPSS version 13.0 software (SPSS, Chicago, Illinois, USA).

3. Results

3.1. Different trends of leaf hydraulic safety margin under normal and extreme droughts

During the normal dry season, all the 16 woody species had positive values for their leaf hydraulic safety margin, with half of them showing values larger than 1 MPa (Fig. 2a). During the extreme dry season, leaf hydraulic safety margin decreased in 13 of the 16 species compared to that during the normal dry season, with the evergreen tree species *Cleistanthus sumatranus* showing the most negative value (–4.12 MPa; Table S1). In contrast, the value for two brevi-deciduous tree species (*Cipadessa baccifera* (Roth.) Miq. and *Ficus pisocarpa*) and a liana species (*Gnetum montanum*) remained unchanged.

There was no significant difference in average $HSM_{\mathrm{leaf\_normal}}$ among evergreen trees, brevi-deciduous trees and lianas ($F_{2,13} = 2.56$, $P > 0.05$; Fig. 2b). Compared to $HSM_{\mathrm{leaf\_normal}}$, the average $HSM_{\mathrm{leaf\_extreme}}$ of evergreen trees substantially decreased to –1.26 MPa. However, $HSM_{\mathrm{leaf\_extreme}}$ and $HSM_{\mathrm{leaf\_normal}}$ did not differ significantly for both brevi-deciduous trees and lianas (Fig. 2b).

3.2. Correlations between hydraulic traits and $HSM_{\mathrm{leaf\_extreme}}$

Across the 16 woody species, $HSM_{\mathrm{leaf\_extreme}}$ was significantly correlated with ρ_{sapwood}, *SWC*, and Ψ_{tlp} (Fig. 3). Species with lower ρ_{sapwood}, higher *SWC*, and Ψ_{tlp} tended to have a larger leaf hydraulic safety margin in the extreme dry season. However, $HSM_{\mathrm{leaf\_extreme}}$ was not significantly correlated with $P50_{\mathrm{leaf}}$ and $P50_{\mathrm{branch}}$ (Table S2).

3.3. Correlations among different calculations of hydraulic safety margins

There was a large inter-specific variation in HSM_{stomatal} and $HSM_{\mathrm{segmentation}}$ across the 16 karst species (Fig. S4). On average, evergreen trees showed larger HSM_{stomatal} and $HSM_{\mathrm{segmentation}}$ than lianas, while there was no significant difference between brevi-deciduous and the other two groups (Fig. S4). Across species, $HSM_{\mathrm{leaf\_normal}}$ was not significantly correlated with HSM_{stomatal}, $HSM_{\mathrm{segmentation}}$, and $HSM_{\mathrm{leaf\_extreme}}$. Similarly, no significant relationship was found between HSM_{stomatal} and $HSM_{\mathrm{leaf\_extreme}}$ (Fig. 4). However, $HSM_{\mathrm{segmentation}}$ was significantly correlated with HSM_{stomatal} and $HSM_{\mathrm{leaf\_extreme}}$. Species with smaller (more negative) $HSM_{\mathrm{segmentation}}$ tended to have smaller HSM_{stomatal} but larger $HSM_{\mathrm{leaf\_extreme}}$ (Fig. 4).

4. Discussion

4.1. Contrasting pattern of leaf hydraulic safety margins across plant groups between the normal and extreme dry seasons

During the normal dry season (modest drought), the evergreen trees showed the largest $HSM_{\mathrm{leaf\_normal}}$ among the three plant groups, partially due to the high resistance to cavitation in their leaf hydraulic systems. Compared to the other two plant groups, the combination of a series of hydraulic characteristics in evergreen trees, i.e., lower $P50_{\mathrm{branch}}$ and $P50_{\mathrm{leaf}}$, higher ρ_{sapwood}, and larger leaf and stomatal hydraulic safety margin (Table S1), exhibited a ‘conservative’ hydraulic adaptation to the dry karst environment (Fu et al., 2012; Zhu et al., 2017). However, this trend was reversed during the extreme drought period, with the evergreen trees showing a high risk of leaf hydraulic failure, as indicated by more negative $HSM_{\mathrm{leaf\_extreme}}$ (Fig. 2b). Particularly, the three dominant evergreen tree species *Celtis philippensis, Cleistanthus sumatranus* and *Lasiococca comberi* showed complete loss of leaf hydraulic conductance, which was consistent with the observation of their extensive leaf desiccation and/or shoot dieback under extreme drought (Fu, 2011).

In contrast, brevi-deciduous trees and lianas showed a positive leaf hydraulic safety margin even under extreme drought conditions (Fig. 2b). These contrasting patterns among plant groups might be associated with their different hydraulic characteristics or strategies dealing with drought. Karst evergreen trees relied primarily on higher cavitation-resistance to survive under drought and might lack other compensatory and effective hydraulic strategies (e.g., deciduousness, stem water storage and deep roots). Previous studies have found that species with high wood density (more resistant to cavitation) tended to experience greater canopy dieback and/or mortality rates under extreme drought (Hoffmann et al., 2011; Kukowski et al., 2013), because denser wood was associated with lower water storage and more negative minimum water potential (Table S2; Meinzer et al., 2009), and thus lower leaf hydraulic safety margin (Fig. 3a, b). In addition, Chen et al. (2015) measured water status and examined the spatial partitioning of soil water use (based on analysis of xylem and soil hydrogen isotope composition) for 25 co-occurring karst tree and liana species in the same karst forest and drought period; and their results indicated that karst evergreen trees absorbed water from shallower soil

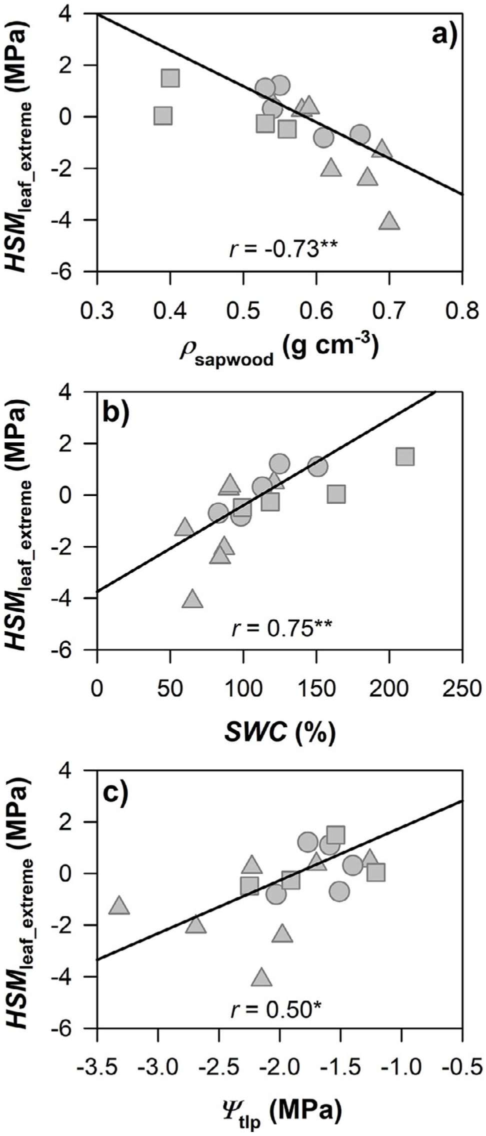

Fig. 3. Correlations between hydraulic traits and leaf hydraulic safety margins during the extreme dry season ($HSM_{\mathrm{leaf\_extreme}}$) across species. Trait abbreviations: ρ_{sapwood}, sapwood density; *SWC*, sapwood saturated water content; Ψ_{tlp}, turgor loss point. Symbols: ***triangle***, evergreen trees; ***circle***, brevi-deciduous trees; ***square***, lianas. Data are the mean value of each species. The solid lines represent linear regression, and Pearson correlation coefficients (*r*) and statistical significance (*P*) are also reported. *, $P < 0.05$; **, $P < 0.01$.

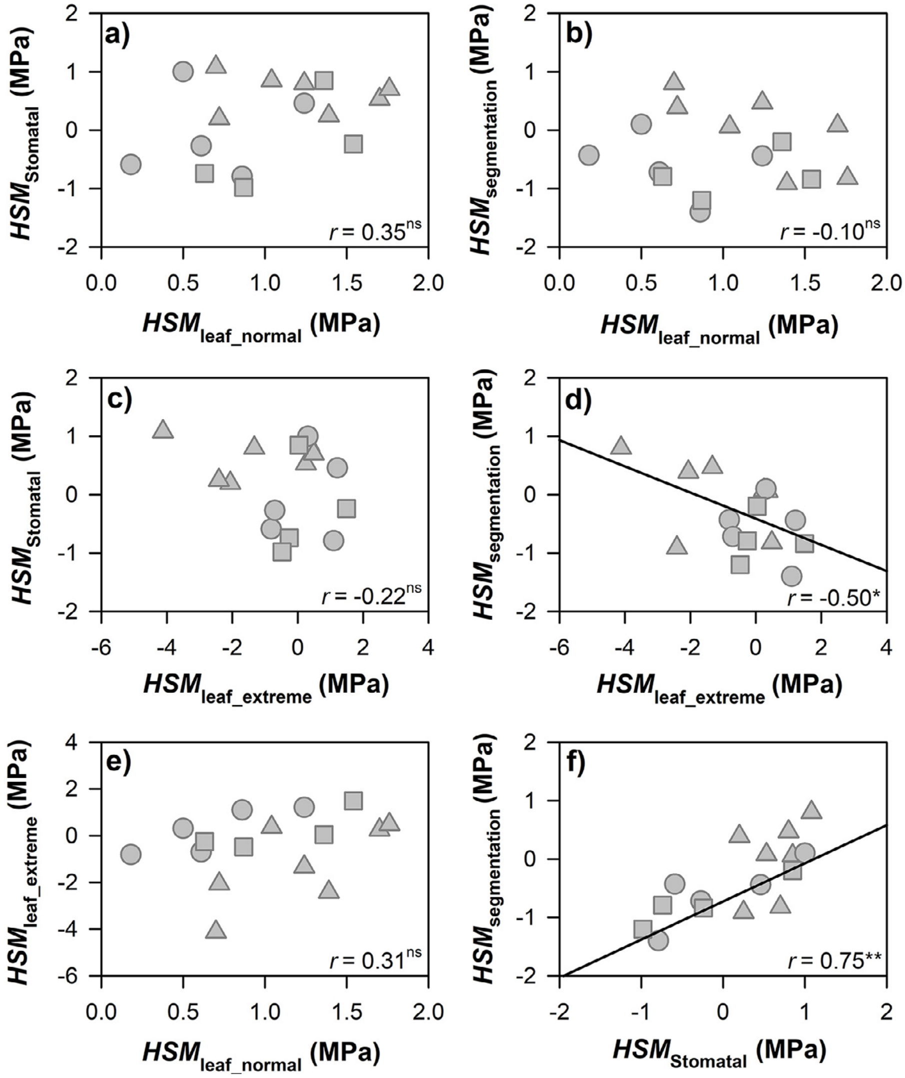

Fig. 4. Correlations among leaf hydraulic safety margins during the normal and extreme dry seasons (HSM_{leaf_normal} and $HSM_{leaf\_extreme}$), stomatal hydraulic safety margin ($HSM_{stomatal}$) and leaf-to-branch vulnerability segmentation ($HSM_{segmentation}$) across the 16 woody species. Data are the mean value of each species. Symbols: *triangle*, evergreen trees; *circle*, brevi-deciduous trees; *square*, lianas. The solid lines represent linear regression, and Pearson correlation coefficients (r) and statistical significance (P) are also reported. *ns,* $P > 0.05$; *, $P < 0.05$; **, $P < 0.01$.

layers and showed more negative predawn leaf water potential compared to lianas (Chen et al., 2015). In contrast, although semi-deciduous trees and lianas were less drought-resistant (Table S1), they could avoid catastrophic cavitation via diverse hydraulic strategies involving leaf shedding, high water storage within the plant body (Ishida et al., 2010), or perhaps greater rooting depth to absorb water sources from deep soils and bedrock layers (Huang et al., 2011; Liu et al., 2011; Chen et al., 2015; Gu et al., 2015). Therefore, they maintained a relatively higher minimum water potential and thus a larger leaf hydraulic safety margin.

Both $P50_{leaf}$ safety margin ($\Psi_{min} - P50_{leaf}$) and $P88_{leaf}$ safety margin ($\Psi_{min} - P88_{leaf}$) are commonly used indices of leaf-level hydraulic safety margins. However, previous studies have indicated that species have an ability to recover from 50% loss of leaf hydraulic conductance, but are not likely to recover from 88% loss of leaf hydraulic conductance (Blackman et al., 2009; Scholz et al., 2014). Therefore, $P88_{leaf}$ safety margin represents hydraulic risks of a plant species to irreversible hydraulic failure under extreme drought, and is a better predictor of drought-induced mortality than $P50_{leaf}$ safety margin, as evident in temperate tree species (Scholz et al., 2014). In this study, $P50_{leaf}$ and $P88_{leaf}$ safety margin showed a significant linear relationship, with more negative $P50_{leaf}$ safety margin (e.g., karst evergreen tree species) also showing narrower or negative $P88_{leaf}$ safety margin (Fig. S3). We suggest that $P50_{leaf}$ can be used as a threshold value of hydraulic risk for karst species under drought in this study, and recommend that both types of safety margins are calculated in future studies.

The difference in hydraulic response of woody plant species between normal and extreme dry seasons has also been documented in other biomes, such as tropical forests (Rice et al., 2004; Ziegler et al., 2019), temperate deciduous forests (Hoffmann et al., 2011), and semi-arid chaparrals (Venturas et al., 2016). These findings further highlight the importance of integrating long-term monitoring of water potential (especially in extreme droughts) with measurement of cavitation resistance and hydraulic safety margins, which provides a more precise estimation of potential hydraulic risk in response to climate change (Bhaskar and Ackerly, 2006; Choat et al., 2012, 2018).

4.2. Correlations between different HSM-calculations

We found no correlation between $HSM_{stomatal}$ and leaf hydraulic safety margin (Fig. 4a, c). During the normal dry season, all the species maintained minimum water potential higher than $P50_{leaf}$ and Ψ_{tlp} (Table S1), which contributed to a positive leaf hydraulic safety margin that did not rely on complete stomatal closure. When extreme drought happens, stomatal closure is not sufficient to maintain water potential within a safe range (Brodribb et al., 2016), as in the case of the evergreen tree species in this study. Leaf water potential may continue to decrease after stomatal closure, becoming more negative as water is lost through cuticular conductance, stomatal leakiness, and other tissues (Choat et al., 2018). Therefore, a hydraulic safety margin determined from the minimum water potential, instead of the water potential associated with stomatal closure, enables a robust estimation of hydraulic risk across species and biomes under extreme droughts (Delzon and Cochard, 2014).

There was a strong correlation between $HSM_{\mathrm{segmentation}}$ and HSM_{stomatal}, species with strong leaf-branch vulnerability segmentation (positive and large $HSM_{\mathrm{segmentation}}$) had large HSM_{stomatal} (Fig. 4f), supporting leaf's functioning as hydraulic bottlenecks and as safety valves to cope with drought (Sack and Holbrook, 2006; Pivovaroff et al., 2014). In this study, a large proportion of species, however, showed negative $HSM_{\mathrm{segmentation}}$ (Fig. 4f). This finding and that of other studies (Bucci et al., 2008; McCulloh et al., 2012; Skelton et al., 2017b) did not support the classic vulnerability segmentation hypothesis. In a previous study, Zhu et al. (2016) indicated that species lacking vulnerability segmentation might have a series of effective hydraulic strategies to maintain water potential within a safe range. Similarly, in another study carried out in a South American temperate forest, Scholz et al. (2014) also found that co-occurring tree species with narrow $HSM_{\mathrm{segmentation}}$ exhibited different physiological mechanisms (e.g., high capacitance, strong stomatal control, and ability to recover hydraulic conductivity) to maintain the water potential far from the threshold of leaf hydraulic failure under extreme drought, leading to large $HSM_{\mathrm{leaf\_extreme}}$ and low mortality rate. Hence, it could be expected that the tree species of the present study with larger $HSM_{\mathrm{segmentation}}$ tended to show more negative $HSM_{\mathrm{leaf\_extreme}}$, and that most of them were evergreen trees (Fig. 4d).

It should be noted that the reliable measurements of $P50_{\mathrm{branch}}$ and $P50_{\mathrm{leaf}}$ are essential for this study because all *HSM*-calculations were based on these two key traits. A number of studies have questioned the reliability of the traditional technique for measuring branch vulnerability curves (Cochard et al., 2013; Wheeler et al., 2013). There might be potential artefact of data in our bench-drying measurements, e.g., flushing of branch segments may refill permanent embolized vessels, and the excision artifact could not be fully excluded for several liana species with a long maximum vessel length. This might lead to overestimation of vulnerability to cavitation in branches for these species. In addition, we did not consider the contribution of extra-vascular pathway (rather than xylem cavitation) to the decline of leaf hydraulic conductance during leaf dehydration (e.g., cell shrinkage; Trifilo et al., 2016), but this might have a minimal influence on the comparison of leaf hydraulic safety margin between normal and extreme droughts. It is therefore recommended that an additional method should be conducted to jointly determine leaf and branch vulnerability to cavitation for these tropical karst species (e.g., optical technique; Brodribb et al., 2016; Skelton et al., 2018).

It should also be noted that the measurements of hydraulic traits (except for leaf water potential) were conducted in a normal dry season and on healthy individuals that had survived the 2008–2012 extreme droughts. Such post-drought measurements to explain plant performance during the extreme drought (e.g., hydraulic risks, dieback, and mortality) are common in many previous studies (Hoffmann et al., 2011; Nardini et al., 2013; Fontes et al., 2018). However, hydraulic traits determined in the normal dry season might be different from those measured under extreme droughts, especially for individuals killed by drought (Tng et al., 2018). Thus these data should be treated with caution (Johnson et al., 2018).

4.3. Implications for predicting community dynamics

For any given forest community, predicting which species are more likely to survive under drought is a central challenge in ecology (Pivovaroff et al., 2016). In this tropical karst forest, our results showed that under extreme droughts evergreen trees experience leaf hydraulic failure more easily compared to brevi-deciduous trees and lianas. With an increasing dry climate in southwestern China (Qiu, 2010; Fan et al., 2011; Fan and Thomas, 2013), it can be speculated that the tropical karst forests will transition from a plant community dominated by large evergreen trees (high hydraulic risk) to the one dominated by a cohort of deciduous trees and lianas (Aguirre-Gutierrez et al., 2019). In addition, we found that $HSM_{\mathrm{leaf\_extreme}}$ was significantly associated with Ψ_{tlp} and ρ_{sapwood} (Fig. 3a, c). This supported the findings of Fu and Meinzer (2018) who suggested that these two easily measured traits were powerful proxies for mechanistic modeling of specific-specific response to increasing droughts. Further, Li et al. (2015) explored the relationships between a series of hydraulic traits (including Ψ_{tlp} and ρ_{sapwood}) and 32-year abundance dynamics of 48 tree species from a permanent subtropical forest plot and indicated that species with higher (less negative) Ψ_{tlp} and lower ρ_{sapwood} increased their abundance with climate change. Relationships between hydraulic traits and demographic rates in the tropical karst forest community could be further analyzed to test our prediction.

5. Conclusions

This study reveals different patterns of HSM_{leaf} in woody species during normal and extreme dry seasons in the tropical karst forest. Evergreen tree species have the largest HSM_{leaf} in the normal dry season but are more likely to undergo hydraulic failure when extreme droughts occur. However, brevi-deciduous trees and lianas could maintain positive HSM_{leaf} in both normal and extreme dry seasons. Species with strong leaf-branch vulnerability segmentation tended to have large stomatal safety margin but smaller (or negative) HSM_{leaf} under extreme drought. Accurate determination of hydraulic traits and linking these traits to species demographic rates (e.g., growth, mortality, and reproductive rates) in the tropical karst forests are recommended in further studies.

Declaration of Competing Interest

All authors contributed critically to the paper and gave final approval for publication.

The authors declare that they have no known competing financial interests or personal relationships that could have appeared to influence the work reported in this paper.

Acknowledgements

We are grateful to Hong Ma and Jia Wen for assistance with field work. We also thank the anonymous reviewers for their constructive comments on the manuscript. This study was funded by the National Natural Science Foundation of China (31470468), the Natural Science Foundation of Guangxi Zhuang Autonomous Region (2018GXNSFAA294027), the grant of Guangxi Key Research and Development Program (Guike AB16380254), the Bagui Young Scholarship of Guangxi Zhuang Autonomous Region, and the Scientific Research Foundation of Guangxi University (XTZ160182). The authors declare no conflicts of interest.

Supplementary materials

Supplementary material associated with this article can be found, in the online version, at doi:10.1016/j.agrformet.2020.108107.

References

Aguirre-Gutierrez, J., Oliveras, I., Rifai, S., Fauset, S., Adu-Bredu, S., Affum-Baffoe, K., et al., 2019. Drier tropical forests are susceptible to functional changes in response to a long-term drought. Ecol. Lett. 22, 855–865.

Allen, C.D., Macalady, A.K., Chenchouni, H., Bachelet, D., McDowell, N., Vennetier, M., et al., 2010. A global overview of drought and heat-induced tree mortality reveals emerging climate change risks for forests. For. Ecol. Manag. 259, 660–684.

Anderegg, W.R.L., Kane, J.M., Anderegg, L.D.L., 2013. Consequences of widespread tree mortality triggered by drought and temperature stress. Nat. Clim. Change 3, 30–36.

Anderegg, W.R.L., Klein, T., Bartlett, M., Sack, L., Pellegrini, A.F.A., Choat, B., Jansen, S., 2016. Meta-analysis reveals that hydraulic traits explain cross-species patterns of drought-induced tree mortality across the globe. Proc. Natl. Acad. Sci. U. S. A. 113, 5024–5029.

Bartlett, M.K., Klein, T., Jansen, S., Choat, B., Sack, L., 2016. The correlations and sequence of plant stomatal, hydraulic, and wilting responses to drought. Proc. Natl. Acad. Sci. U. S. A. 113, 13098–13103.

Bhaskar, R., Ackerly, D.D., 2006. Ecological relevance of minimum seasonal water potentials. Physiol. Plantarum 127, 353–359.

Blackman, C.J., Brodribb, T.J., Jordan, G.J., 2009. Leaf hydraulics and drought stress: response, recovery and survivorship in four woody temperate plant species. Plant Cell Environ. 32, 1584–1595.

Blackman, C.J., Creek, D., Maier, C., Aspinwall, M.J., Drake, J.E., Pfautsch, S., et al., 2019. Drought response strategies and hydraulic traits contribute to mechanistic understanding of plant dry-down to hydraulic failure. Tree Physiol. 39, 910–924.

Booth, R.K., Jackson, S.T., Sousa, V.A., Sullivan, M.E., Minckley, T.A., Clifford, M.J., 2012. Multi-decadal drought and amplified moisture variability drove rapid forest community change in a humid region. Ecology 93, 219–226.

Brodribb, T.J., Holbrook, N.M., 2003. Stomatal closure during leaf dehydration, correlation with other leaf physiological traits. Plant Physiol. 132, 2166–2173.

Brodribb, T.J., Holbrook, N.M., 2004. Stomatal protection against hydraulic failure: a comparison of coexisting ferns and angiosperms. New Phytol. 162, 663–670.

Brodribb, T.J., Holbrook, N.M., Edwards, E.J., Gutierrez, M.V., 2003. Relations between stomatal closure, leaf turgor and xylem vulnerability in eight tropical dry forest trees. Plant Cell Environ. 26, 443–450.

Brodribb, T.J., Skelton, R.P., McAdam, S.A.M., Bienaime, D., Lucani, C.J., Marmottant, P., 2016. Visual quantification of embolism reveals leaf vulnerability to hydraulic failure. New Phytol. 209, 1403–1409.

Bucci, S.J., Goldstein, G., Meinzer, F.C., Scholz, F.G., Franco, A.C., Bustamante, M., 2004. Functional convergence in hydraulic architecture and water relations of tropical savanna trees: from leaf to whole plant. Tree Physiol. 24, 891–899.

Bucci, S.J., Scholz, F.G., Goldstein, G., Meinzer, F.C., Franco, A.C., Zhang, Y., Hao, G.Y., 2008. Water relations and hydraulic architecture in Cerrado trees: adjustments to seasonal changes in water availability and evaporative demand. Braz. J. Plant Physiol. 20, 233–245.

Bucci, S.J., Scholz, F.G., Peschiutta, M.L., Arias, N.S., Meinzer, F.C., Goldstein, G., 2013. The stem xylem of Patagonian shrubs operates far from the point of catastrophic dysfunction and is additionally protected from drought-induced embolism by leaves and roots. Plant Cell Environ. 36, 2163–2174.

Bucci, S.J., Carbonell Silletta, L.M., Garre, A., Cavallaro, A., Efron, S.T., Arias, N.S., Goldstein, G., Scholz, F.G., 2019. Functional relationships between hydraulic traits and the timing of diurnal depression of photosynthesis. Plant Cell Environ. 42, 1603–1614.

Chen, Y.J., Cao, K.F., Schnitzer, S.A., Fan, Z.X., Zhang, J.L., Bongers, F., 2015. Water-use advantage for lianas over trees in tropical seasonal forests. New Phytol. 205, 128–136.

Choat, B., Lahr, E.C., Melcher, P.J., Zwieniecki, M.A., Holbrook, N.M., 2005. The spatial pattern of air seeding thresholds in mature sugar maple trees. Plant Cell Environ. 28, 1082–1089.

Choat, B., Jansen, S., Brodribb, T.J., Cochard, H., Delzon, S., Bhaskar, R., et al., 2012. Global convergence in the vulnerability of forests to drought. Nature 491, 752–755.

Choat, B., Brodribb, T.J., Brodersen, C.R., Duursma, R.A., Lopez, R., Medlyn, B.E., 2018. Triggers of tree mortality under drought. Nature 588, 531–539.

Cochard, H., Badel, E., Herbette, S., Delzon, S., Choat, B., Jansen, S., 2013. Methods for measuring plant vulnerability to cavitation: a critical review. J. Exp. Bot. 64, 4779–4791.

Delzon, S., Cochard, H., 2014. Recent advances in tree hydraulics highlight the ecological significance of the hydraulic safety margin. New Phytol. 203, 355–358.

Fan, D.Y., Jie, S.L., Liu, C.C., Zhang, X.Y., Xu, X.W., Zhang, S.R., Xie, Z.Q., 2011a. The trade-off between safety and efficiency in hydraulic architecture in 31 woody species in a karst area. Tree Physiol. 31, 865–877.

Fan, Z.X., Brauning, A., Thomas, A., Li, J.B., Cao, K.F., 2011b. Spatial and temporal temperature trends on the Yunnan Plateau (Southwest China) during 1961-2004. Int. J. Climatol. 31, 2078–2090.

Fan, Z.X., Thomas, A., 2013. Spatiotemporal variability of reference evapotranspiration and its contributing climatic factors in Yunnan Province, SW China, 1961-2004. Clim. Change 116, 309–325.

Feng, X., Porporato, A., Rodriguez-Iturbe, I., 2013. Changes in rainfall seasonality in the tropics. Nat. Clim. Change 3, 811–815.

Fontes, C.G., Dawson, T.E., Jardine, K., McDowell, N., Gimenez, B.O., Anderegg, L., et al., 2018. Dry and hot: the hydraulic consequences of a climate change-type drought for Amazonian trees. Phil. Trans. R. Soc. B 373, 20180209.

Fu, P.L., 2011. Contrasting Stem Hydraulic Traits, Water Relations and Photosynthesis Between Evergreen and Deciduous Trees in a Tropical Karst Forest. Chinese Academy of Sciences PhD thesis.

Fu, P.L., Jiang, Y.J., Wang, A.Y., Brodribb, T.J., Zhang, J.L., Zhu, S.D., Cao, K.F., 2012. Stem hydraulic traits and leaf water-stress tolerance are co-ordinated with the leaf phenology of angiosperm trees in an Asian tropical dry karst forest. Ann. Bot. 110, 189–199.

Fu, X., Meinzer, F., 2018. Metrics and proxies for stringency of regulation of plant water status (iso/anisohydry): a global data set reveals coordination and tradeoffs among water transport traits. Tree Physiol. 39, 122–134.

Gu, D., Zhang, Z., Mallik, A., Zhou, A., Mo, L., He, C., Huang, Y., 2015. Seasonal water use strategy of *Cyclobalanopsis glauca* in a karst area of southern China. Environ. Earth Sci 74, 1007–1014.

Hoffmann, W.A., Marchin, R.M., Abit, P., Lau, O.L., 2011. Hydraulic failure and tree dieback are associated with high wood density in a temperate forest under extreme drought. Global Change Biol. 17, 2731–2742.

Huang, Y., Li, X., Zhang, Z., He, C., Zhao, P., You, Y., Mo, L., 2011. Seasonal changes in *Cyclobalanopsis glauca* transpiration and canopy stomatal conductance and their dependence on subterranean water and climatic factors in rocky karst terrain. J. Hydrol. 402, 135–143.

Ishida, A., Harayama, H., Yazaki, K., Ladpala, P., Sasrisang, A., Kaewpakasit, K., et al., 2010. Seasonal variations of gas exchange and water relations in deciduous and evergreen trees in monsoonal dry forests of Thailand. Tree Physiol. 30, 935–945.

Johnson, D.M., McCulloh, K.A., Meinzer, F.C., Woodruff, D.R., Eissenstat, D.M., 2011. Hydraulic patterns and safety margins, from stem to stomata, in three eastern U.S. tree species. Tree Physiol. 31, 659–668.

Johnson, D.M., Wortemann, R., McCulloh, K.A., Jordan-Meille, L., Ward, E.J., Warren, J.M., et al., 2016. A test of the hydraulic vulnerability segmentation hypothesis in angiosperm and conifer tree species. Tree Physiol. 36, 983–993.

Johnson, D.M., Domec, J.C., Berry, Z.C., Schwantes, A.M., McCulloh, K.A., Woodruff, D.R., et al., 2018. Co-occurring woody species have diverse hydraulic strategies and mortality rates during an extreme drought. Plant Cell Environ. 41, 576–588.

Klein, T., Yakir, D., Buchmann, N., Grunzweig, J.M., 2014. Towards an advanced assessment of the hydrological vulnerability of forests to climate change-induced drought. New Phytol. 201, 712–716.

Kukowski, K.R., Schwinning, S., Schwartz, B.F., 2013. Hydraulic response to extreme drought conditions in three co-dominant tree species in shallow soil over bedrock. Oecologia 171, 819–830.

Lambers, H., ChapinIII, F.S., Pons, T.L., 2008. Plant Physiological Ecology, 2nd edition. Springer, New York.

Li, R., Zhu, S., Chen, H.Y.H., John, R., Zhou, G., Zhang, D., Zhang, Q., Ye, Q., 2015. Are functional traits a good predictor of global change impacts on tree species abundance dynamics in a subtropical forest? Ecol. Lett. 18, 1181–1189.

Liu, C.C., Liu, Y.G., Guo, K., Li, G.Q., Zheng, Y.R., Yu, L.F., Yang, R., 2011. Comparative ecophysiological responses to drought of two shrub and four tree species from karst habitats of southwestern China. Trees 25, 537–549.

Liu, Y.Y., Wang, A.Y., An, Y.N., Lian, P.Y., Wu, D.D., Zhu, J.J., et al., 2018. Hydraulics play an important role in causing low growth rate and dieback of aging Pinus sylvestris var. mongolica trees in plantations of Northeast China. Plant Cell Environ. 41, 1500–1511.

Martin-StPaul, N., Delzon, S., Cochard, H., 2017. Plant resistance to drought depends on timely stomatal closure. Ecol. Lett. 20, 1437–1447.

McDowell, N., Pockman, W.T., Allen, C.D., Breshears, D.D., Cobb, N., Kolb, T., Plaut, J., Sperry, J., West, A., Williams, D.G., Yepez, E.A., 2008. Mechanisms of plant survival and mortality during drought: why do some plants survive while others succumb to drought? New Phytol. 178, 719–739.

McCulloh, K.A., Johnson, D.M., Meinzer, F.C., Voelker, S.L., Lachenbruch, B., Domec, J.C., 2012. Hydraulic architecture of two species differing in wood density: opposing strategies in co-occurring tropical pioneer trees. Plant Cell Environ. 35, 116–125.

McCulloh, K.A., Johnson, D.M., Petitmermet, J., McNellis, B., Meinzer, F.C., Lachenbruch, B., 2015. A comparison of hydraulic architecture in three similarly sized woody species differing in their maximum potential height. Tree Physiol. 35, 723–731.

Meinzer, F.C., Johnson, D.M., Lachenbruch, B., McCulloh, K.A., Woodruff, D.R., 2009. Xylem hydraulic safety margins in woody plants: coordination of stomatal control of xylem tension with hydraulic capacitance. Funct. Ecol. 23, 922–930.

Nardini, A., Battistuzzo, M., Savi, T., 2013. Shoot desiccation and hydraulic failure in temperate woody angiosperms during an extreme summer drought. New Phytol. 200, 322–329.

Nolf, M., Creek, D., Duursma, R., Holtum, J., Mayr, S., Choat, B., 2015. Stem and leaf hydraulic properties are finely coordinated in three tropical rainforest tree species. Plant Cell Environ. 38, 2652–2661.

Pivovaroff, A.L., Cook, V.M.W., Santiago, L.S., 2018. Stomatal behaviour and stem xylem traits are coordinated for woody plant species under exceptional drought conditions. Plant Cell Environ. 41, 2617–2626.

Pivovaroff, A.L., Pasquini, S.C., De Guzman, M.E., Alstad, K.P., Stemke, J.S., Santiago, L.S., 2016. Multiple strategies for drought survival among woody plant species. Funct. Ecol. 30, 517–526.

Pivovaroff, A.L., Sack, L., Santiago, L.S., 2014. Coordination of stem and leaf hydraulic conductance in southern California shrubs: a test of the hydraulic segmentation hypothesis. New Phytol. 203, 842–850.

Powers, J.S., Vargas, G.G., Brodribb, T.J., Schwartz, N.B., Pérez-Aviles, D., Smith-Martin, C.M., et al., 2020. A catastrophic tropical drought kills hydraulically vulnerable tree species. Global Change Biol. 26, 3122–3133.

Qiu, J., 2010. China drought highlights future climate threats. Nature 465, 142–143.

Rice, K.J., Matzner, S.L., Byer, W., Brown, J.R., 2004. Patterns of tree dieback in Queensland, Australia: the importance of drought stress and the role of resistance to cavitation. Oecologia 139, 190–198.

Rowland, L., da Costa, A.C.L., Galbraith, D.R., Oliveira, R.S., Binks, O.J., Oliveira, A.A.R., et al., 2015. Death from drought in tropical forests is triggered by hydraulics not carbon starvation. Nature 528, 119–122.

Sack, L., Holbrook, N.M., 2006. Leaf hydraulics. Annu. Rev. Plant Biol. 57, 361–381.

Scholz, F.G., Bucci, S.J., Goldstein, G., 2014. Strong hydraulic segmentation and leaf senescence due to dehydration may trigger die-back in *Nothofagus dombeyi* under severe droughts: a comparison with the co-occurring *Austrocedrus chilensis*. Trees 28, 1475–1487.

Schulte, P.J., Hinckley, T.M., 1985. A comparison of pressure-volume curve data analysis techniques. J. Exp. Bot. 36, 590–602.

Skelton, R.P., West, A.G., Dawson, T.E., 2015. Predicting plant vulnerability to drought in biodiverse regions using functional traits. Natl. Acad. Sci. U S A 112, 5744–5749.

Skelton, R.P., Brodribb, T.J., McAdam, S.A.M., Mitchell, P.J., 2017a. Gas exchange recovery following natural drought is rapid unless limited by loss of leaf hydraulic conductance: evidence from an evergreen woodland. New Phytol. 215, 1399–1412.

Skelton, R.P., Brodribb, T.J., Choat, B., 2017b. Casting light on xylem vulnerability in an herbaceous species reveals a lack of segmentation. New Phytol. 214, 561–569.

Skelton, R.P., Dawson, T.E., Thompson, S.E., Shen, Y., Weitz, A.P., Ackerly, D., 2018. Low vulnerability to xylem embolism in leaves and stems of North American oaks. Plant Physiol. 177, 1066–1077.

Sperry, J.S., Donnelly, J.R., Tyree, M.T., 1988. A method for measuring hydraulic conductivity and embolism in xylem. Plant Cell Environ. 1, 35–40.

Tng, D.Y.P., Apgaua, D.M.G., Ishida, Y.F., Mencuccini, M., Lloyd, J., Laurance, W.F., Laurance, S.G.W., 2018. Rainforest trees respond to drought by modifying their hydraulic architecture. Ecol. Evol. 8, 12479–12491.

Trifilo, P., Raimondo, F., Savi, T., Lo Gullo, M.A., Nardini, A., 2016. The contribution of vascular and extra-vascular water pathways to drought-induced decline of leaf hydraulic conductance. J. Exp. Bot. 67, 5029–5039.

Trueba, S., Pan, R., Scoffoni, C., John, G.P., Davis, S.D., Sack, L., 2019. Thresholds for leaf damage due to dehydration: declines of hydraulic function, stomatal conductance and cellular integrity precede those for photochemistry. New Phytol. 223, 134–149.

Tyree, M.T., Cochard, H., Cruiziat, P., Sinclair, B., Ameglio, T., 1993. Drought-induced leaf shedding in walnut: evidence for vulnerability segmentation. Plant Cell Environ. 16, 879–882.

Venturas, M.D., MacKinnon, E.D., Dario, H.L., Jacobsen, A.L., Pratt, R.B., Davis, S.D., 2016. Chaparral shrub hydraulic traits, size, and life history types relate to species mortality during California's historic drought of 2014. PLoS ONE 11, e0159145.

Wason, J.W., Anstreicher, K.S., Stephansky, N., Huggett, B.A., Brodersen, C.R., 2018. Hydraulic safety margins and air-seeding thresholds in roots, trunks, branches and petioles of four northern hardwood trees. New Phytol. 219, 77–88.

Wheeler, J.K., Huggett, B.A., Tofte, A.N., Rockwell, F.E., Holbrook, N.M., 2013. Cutting xylem under tension or supersaturated with gas can generate PLC and the appearance of rapid recovery from embolism. Plant Cell Environ. 36, 1938–1949.

Yuan, D.X., 1991. Karst of China. Geological Publishing House, Beijing.

Zhang, S.B., Zhang, J.L., Cao, K.F., 2017. Divergent hydraulic safety strategies in three co-occurring Anacardiaceae tree species in a Chinese savanna. Front. Plant Sci. 7, 2075.

Zhang, X., Zwiers, F.W., Hegerl, G.C., Lambert, F.H., Gillett, N.P., Solomon, S., et al., 2007. Detection of human influence on twentieth-century precipitation trends. Nature 448, 461–465.

Zhu, H., Wang, H., Li, B., Sirirugsa, P., 2003. Biogeography and floristic affinities of the limestone flora in southern yunnan. China. Ann. Mo. Bot. Gard. 90, 444–465.

Zhu, S.D., Liu, H., Xu, Q.Y., Cao, K.F., Ye, Q., 2016. Are leaves more vulnerable to cavitation than branches? Funct. Ecol. 30, 1740–1744.

Zhu, S.D., Chen, Y.J., Fu, P.L., Cao, K.F., 2017. Different hydraulic traits of woody plants from tropical forests with contrasting soil water availability. Tree Physiol. 37, 1469–1477.

Ziegler, C., Coste, S., Stahl, C., Delzon, S., Levionnois, S., Cazal, J., et al., 2019. Large hydraulic safety margins protect Neotropical canopy rainforest tree species against hydraulic failure during drought. Ann. For. Sci. 76, 115.